

Generation and detection of ultrabroadband infrared wave exceeding 200 THz

Eiichi Matsubara, Masaya Nagai, and Masaaki Ashida

Graduate School of Engineering Science, 560-8531, Osaka University, Japan

Abstract. By focusing a hollow-fiber compressed intense 10-fs pulse and its second harmonic in air, an ultrabroadband infrared pulse with a spectral range of 1–200 THz is generated through a plasma. Coherent detection of the signal up to 100 THz is achieved with electro-optic sampling and THz air-breakdown-coherent-detection. The drastic dependence on the orientation of the second harmonic crystal is clarified in a range of 100–200 THz. From these, the whole frequency components are confirmed to be generated from the AC biased plasma and phase-locked.

Infrared spectroscopy has been an important tool for material science because the energies of various elementary excitations are contained in this range. Especially in transition metal oxides, optical conductivity spectra continuously range from far to near infrared, reflecting strong correlations between multiple elementary excitations. Hence, in order to fully understand their optical properties, it is crucial to probe the whole frequency range of interest. Although Fourier transform infrared spectroscopy (FTIR) has been mainly employed for such studies, it is difficult to combine with time-resolved pump-probe measurements. Hence, the development of an ultrabroadband coherent optical source has been highly desired, which is also beneficial in the simultaneous determination of the real and imaginary parts of optical constants.

Recently, coherent terahertz pulses have been found to be generated through a plasma induced by focusing an intense ultrashort laser pulse in air [1, 2]. Among many schemes proposed so far, such as DC bias, AC bias (ω - 2ω pumping), few-cycle pulse pumping, and one utilizing a ponderomotive force, the AC bias method seems to be the most efficient. The mechanism has been phenomenologically understood as a four wave optical rectification process. Applying hollow-fiber compressed [3] sub-20-fs pulses to the AC bias method, the infrared wave generation up to 140 THz [4] and the coherent detection up to 70 THz [1] were achieved. In this study, we produce a 400- μ J, 10-fs pulse with the hollow fiber compression and apply it to the AC bias method [5].

In experiments, amplified 35-fs, 1.2–1.8 mJ Ti sapphire laser pulses were loosely focused onto a fused-silica hollow fiber set in an Ar gas filled chamber. The dispersion of the spectrally broadened output pulse with 480–700 μ J energy was compensated for using a pair of chirped mirrors. The pulse profile was characterized with a setup of spectral-phase interferometry for direct electric-field reconstruction (SPIDER). By appropriately adjusting the number of reflections, an intense extremely short pulse with 10-fs duration and 400–600- μ J energy was produced. This pulse was divided with a fused-silica plate or a beamsplitter; the transmission (reflection) serves as the pump (probe) pulse. The pump pulse was focused with an off-axis parabolic mirror together with its second harmonic (SH) which was generated in a 100- μ m thick β -BaB₂O₄ (BBO) crystal set at a distance of 20 mm ahead of the focus. A high resistivity silicon plate cut the residual pump. A monochromator with a

cooled HgCdTe (MCT) detector measured the mid to near infrared spectrum. Time domain measurements were carried out using a conventional electro-optic sampling and a setup of THz air-breakdown-coherent-detection (THz-ABCD) [2] provided by Zomega corporation. In the former a 20- μm thick GaSe crystal served as the detector; GaSe is an advantageous material for high frequency measurements because thin crystals can be obtained by cleaving and phase matching of difference frequency process between mid and near infrared lights can be satisfied [6]. In the latter, infrared pulses generated from the plasma and the probe pulse were focused between electrodes where 20-kV/cm bias was applied. Lock-in detection enabled us to extract the electric-field profile of the infrared pulse through the SH signal of the probe pulse, which a photomultiplier tube detected [2].

Figure 1 shows the intensity spectrum of the infrared pulse measured with the MCT detector. As is seen, the spectrum ranges to 200 THz (1.5 μm). The signal intensity at 150 THz (2 μm) became the maximum when the surface of the BBO crystal was nearly perpendicular to the pump beam, and the extraordinary axis was rotated by 50° from the angle at which the SH intensity was the maximum. Since this is almost the same as that for THz waves in other studies [1,4,7], the present signal seems to originate from the AC biased plasma. The small component which originated from self-phase modulation (SPM) is rising up from 220 THz. To clearly distinguish between the two components, we examined their dependence on the BBO crystal condition. As shown in the inset of Fig. 1, no infrared signal was observed above 100 THz without the BBO crystal but the edge of the SPM component was recognized above 180 THz (dotted curve). At another BBO angle of 10°, a similar spectrum to the 50° case was detected (dashed curve), however, the intensity was 20 times smaller. This drastic BBO crystal dependence indicates that the ultrabroadband infrared pulse originates not from the SPM in air, but from the polarization sensitive four wave mixing (FWM) process.

Next we coherently detected the infrared pulse with time domain spectroscopy. Figure 2 shows the Fourier transformed spectrum of the infrared pulse (solid curve) and the noise curve (dotted curve). The inset shows the temporal electric-field profile. Here we can see the spectrum surely extends to 100 THz. The BBO orientation optimized for the field amplitude was the same as that of the near infrared (>100 THz) signal observed with the MCT detector, supporting the analysis that both the components originated from the same mechanism. Figure 3 shows the result using THz-ABCD, where the Fourier transformed spectrum also extends to 100 THz. Summarizing the results in Figs. 1, 2 and 3, an ultrabroadband coherent infrared pulse covering a continuous frequency range of 1–200 THz is generated. One might still wonder if the 100–200 THz component is truly coherent. However, the possibility of incoherent SPM and Raman effect are ruled out by the drastic dependence on the SH crystal and the smooth spectrum, respectively. The imperfect spectral sensitivity of the time domain measurements is due to the finite duration of the probe pulse and the absence of the carrier-envelope phase (CEP) locking of the pump. Phase-locked generation should be possible in principle, however, the intensity will fluctuate. This fact will account for the “enhanced” noise floor compared with the measured noise floor in Fig. 2. Further compression of the probe pulse and/or CEP locking of the pump will enable the coherent detection in the full range to 200 THz.

In the generation process of the ultrabroadband infrared pulse, not only the duration of the fundamental (ω) pulse, but that of the SH (2ω) pulse is also important. However, it is so difficult to control the 2ω pulse profile independently. Hence, a practical way of controlling it is to change the ω pulse profile. Thus we examined the dependence of the infrared spectrum on the number of reflections on the chirped mirrors. As a result, even when increasing the number of round trips by three, the spectrum did not change so much and the high frequency edge still exceeded 180 THz. In contrast, when reducing it even by once, both the intensity and bandwidth quickly dropped as shown in Fig. 4. This behavior can be explained as follows: the group delay dispersion (GDD) given by the chirped mirrors is -40 fs^2 per round trip and that given by a 100- μm thick BBO crystal is 4.9 fs^2 at 800 nm for extraordinary and 21.8 fs^2 at 400 nm for ordinary. Hence, the 2ω pulse experiences higher GDD than the ω one. In principle, an ultrabroadband infrared pulse can be efficiently generated only when both the ω and 2ω pulses are temporally overlapped so that the achievable bandwidth is determined by the shorter duration of them. Provided the ω pulse is Fourier transform limited before the incidence to the BBO crystal, the 2ω pulse gets more positively chirped after the

BBO crystal so that the “shorter” ω pulse duration determines the bandwidth. By decreasing the reflection even by once, the ω pulse gets positively chirped and the 2ω pulse becomes more stretched, resulting in a rapid decrease in bandwidth. In contrast, by increasing the reflection, the 2ω pulse duration gets narrower for a few additional bounces although the ω pulse duration gets negatively stretched. In this case, the 2ω pulse duration determines the bandwidth, which does not drop so rapidly. From these we find that perfect chirp compensation is not necessarily requisite but some negative chirp is allowed for the broadband infrared pulse generation.

In conclusion, we generated an ultrabroadband coherent infrared pulse with a spectral range of 1–200 THz from an air plasma induced by a hollow-fiber compressed intense 10-fs pulse and its second harmonic. The time domain detection up to 100 THz assures the coherence in the range. The drastic dependence on the orientation of the second harmonic crystal in a range of 100-200 THz confirms that the generation mechanism is the phase-locked FWM.

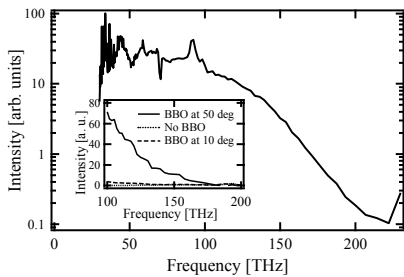


Fig. 1 Spectrum of the infrared pulse observed using monochromator and MCT detector. Inset shows the dependence on the BBO crystal conditions.

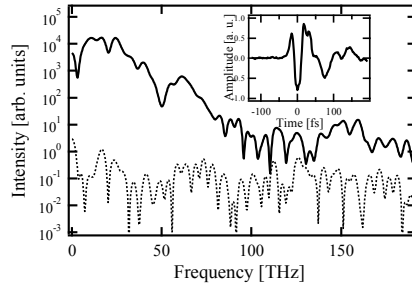


Fig. 2 Fourier transformed spectrum of the infrared pulse observed by electro-optic sampling with 20- μm thick GaSe crystal. Inset shows the temporal electric field profile.

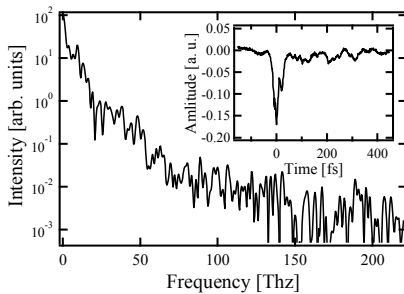


Fig. 3 Fourier transformed spectrum of the infrared pulse observed with THz-ABCD. Inset shows the temporal electric-field profile.

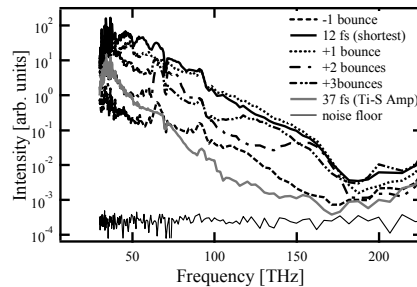


Fig. 4 Dependence of the infrared pulse spectrum on the input pulse profile. Assuming that 12 fs pulse is Fourier transform limited, reflections times on chirped mirrors is decreased or increased. The case of 37-fs laser pulse is also shown.

References

1. M.D. Thomson, M. Krefß, T. Löffler, and H.G. Roskos, *Laser Photon. Rev.* **1**, 349 (2007) and references therein.
2. J. Dai, J. Liu, and X.-C. Zhang, *IEEE J. Sel. Top. Quantum Electron.* **17**, 183(2011) and references therein.
3. M. Nisoli, S. De Silvestri, and O. Svelto, *Appl. Phys. Lett.* **68**, 2793 (1996).
4. M.D. Thomson, V. Blank, and H.G. Roskos, *Opt. Express* **18**, 23173 (2010).
5. E. Matsubara, M. Nagai, and M. Ashida, *Appl. Phys. Lett.* **101**, 011105 (2012).
6. C. Kübler, R. Huber, S. Tubel, and A. Leitenstorfer, *Appl. Phys. Lett.* **85**, 3360 (2004).
7. K. Y. Kim, J. H. Glowonia, A. J. Taylor, and G. Rodriguez, *Opt. Express* **15**, 4577 (2007).